

Impact of Network Load on Forward Link Inter-cell Interference in Cellular Data Networks

Vivek P. Mhatre, *Member, IEEE*, Catherine P. Rosenberg, *Member, IEEE*

Abstract— We study the impact of network load in the neighboring sectors on the inter-cell interference in a cellular data network. The signal received by a user over the forward link in such a system contains interference from the neighboring base stations. We note that the strength of this interference is a function of the network load in the neighboring cells. We obtain an expression for the received SINR (Signal to Interference and Noise Ratio) as a function of the traffic load in the interfering cells. Using this result, we propose an improvement to the conservative pilot-based SINR estimation scheme that is implemented in the current cellular data networks. The proposed scheme provides a more accurate estimate of the user SINR by taking better account of the contribution of inter-cell interference. It builds on top of the current SINR measurement scheme by using a combination of pilot measurement and traffic load measurement. With the proposed scheme, a terminal reports a less conservative data rate, and hence it receives a higher throughput. The scheme especially benefits the “poor” users, i.e., the users that receive low throughput because they are located far from the base station. For example, when the network load in the neighboring sectors is 0.5, with the proposed scheme, the throughput received by a single vehicular user located about three-fourth of the way between the serving base station and the cell boundary, is about 35% higher than the throughput obtained using the scheme that is used in current practice.

Index Terms— Inter-cell interference, cellular networks, CDMA-HDR.

I. INTRODUCTION

CELLULAR data networks allow mobile terminals to access the Internet for data communication. Some examples of such cellular data networks are the CDMA-HDR (High Data Rate) networks [13], and the 1xEVDO (1x Evolution Data and Voice) networks [7]. While our work is applicable to both these systems, as well as other systems that use pilot based channel estimation, henceforth we use CDMA-HDR as our case study. In such networks, the forward link (the link from the base station to the terminals¹) is time domain multiplexed to serve one or more users with the available bandwidth and power. The rate at which a user is served over the forward link is governed by the current channel conditions, i.e., the SINR (Signal to Interference and Noise Ratio) of the user. The user SINR is a function of several factors such as path loss, shadowing, fading, noise, and *inter-cell interference*. The latter is the focus of this work. Inter-cell interference refers to the interference received by a terminal over the forward link

because of the co-channel forward link transmissions of the base stations in the neighboring cells.

We note that the extent of inter-cell interference experienced by a terminal is a function of the network load on the forward link of the neighboring cells. Hence the interference is higher (and the data rate is lower) when the network loads on the interfering forward links are higher, and vice versa. The goal of this work is to study the *cross-layer* impact on the *physical layer* of a terminal in the given cell due to the loads at the *network layer* of the neighboring cells. Our study pertains only to the forward link. The SINR measurement in the current implementations [13], [7] is performed on pilot signals transmitted in a synchronous fashion by all the base stations. In this scheme, the SINR is estimated in a way equivalent to assuming that the forward links of the interfering cells are always busy. However, the forward link of a cell does not carry traffic 100% of the time, and this results in overestimation of the inter-cell interference with this scheme. Although the scheme additionally uses Hybrid-ARQ for early packet termination, user throughput still suffers due to overestimation of interference. We propose a scheme that takes into account the dependence of SINR on the current network loads in the neighboring cells. We illustrate through simulation results that, using our scheme, it is possible to improve the user throughput, especially for the “poor” users, i.e., the users that receive low throughput because they are located far from the base station.

The paper is organized as follows. We first discuss some related work in section II. In section III, we provide an overview of the system model that we study, and the analytical results on the characterization of inter-cell interference. In section IV, we propose an improved scheme for a more accurate estimation of user SINR. We then present an overview of the simulator, and simulation results in section V. Finally, we conclude in section VI.

II. RELATED WORK

In [16], Yoon *et al.* consider the multi-access uplink of a CDMA *voice* network. Due to the lack of perfect orthogonality between the uplink CDMA channels, each user causes interference to other users. The authors find an expression for the characteristic function of the interference component in the received signal. While this work can be extended to the context of inter-cell interference, the method of determining SINR involves several computations, and does not provide insightful results about the exact *dependence of user SINR on the network load in the interfering sectors*.

Manuscript submitted February, 2005; revised July 2005 and January 2006. Vivek P. Mhatre is with Intel Research Labs, Cambridge, UK, and Catherine P. Rosenberg is with the Department of Electrical and Computer Engineering, University of Waterloo, Canada. Email: mhatre@gmail.com, cath@ece.uwaterloo.ca.

¹Henceforth, we use the terms ‘user’ and ‘terminal’ interchangeably.

In [3], Haas *et al.* consider the problem of characterizing the inter-cell interference in CDMA voice networks. The authors consider the problem of characterizing inter-cell interference at the base station of a sector due to a single user transmission in the neighboring sector. In [9], Romero-Jerez *et al.* consider the problem of characterizing intra-cell as well as inter-cell interference for the uplink of a CDMA voice networks. However, as in the case of [16], both these works ([3], [9]) assume continuous transmission of the interfering signal; a characteristic of voice traffic, but not of data traffic. Besides, all these works result in fairly complicated expressions for symbol error probability, and hence cannot be used directly in the SINR estimation procedure implemented at the terminal. Other works such as [15] have studied the effect of inter-cell interference over the forward link, and the benefits of Hybrid-ARQ in countering the interference.

Our work is different from all the above works in that we focus on data networks, and exploit the fact that network load in the interfering sectors strongly influences the interference levels at a given terminal. This observation can be used by the terminal to predict its SINR more accurately as we discuss next.

III. CHARACTERIZING INTER-CELL INTERFERENCE

Our analysis in this section is applicable to any SINR estimation scheme that uses synchronous pilot transmission by the base stations. However, as a case study, we consider a CDMA-HDR system [13]. In such a system, data users are served over a data-only channel. There are no voice users in the system. Each hexagonal cell is divided into three sectors (see Fig. 1). Let R be the radius of the sector. The base station uses a directional antenna for each of the three sectors, and hence we assume that there is no interference from the adjacent sectors of the same cell. However, a user in a given sector receives inter-cell interference from the neighboring sectors of the adjacent cells. For example, in Fig. 1 a user in sector 0 of cell C receives inter-cell interference from sector 1 of cell C' and sector 2 of cell C'' .

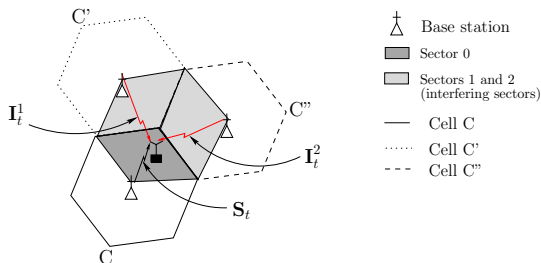


Fig. 1. Inter-cell interference

The users in each sector are served over the forward link in a TDM fashion using all the available power and bandwidth. The forward link is time domain multiplexed into *time slots*. The forward link waveform can be modeled as an ON-OFF process. During the ON time, i.e., during a busy time slot, the base station² sends a sequence of +1 and -1 pulses (*chips*

²Henceforth, BS stands for base station.

in CDMA terminology). During the OFF time, i.e., during an idle time slot, there is no signal. Hence the interference experienced by a user *because* of the forward link signal of a neighboring BS consists of this modified ON-OFF process. The higher the forward link traffic load in the neighboring sector, the greater the inter-cell interference caused by that sector to the users in the given sector.

Referring to Fig. 1, consider a terminal located in sector 0, and let the total forward link inter-cell interference at the terminal as a function of time t be \mathbf{I}_t . Through simple geometric arguments, it is easy to show that the ratio of the distance from the edge of the cell to other interfering base stations (not the two nearest interfering base stations), is at least twice the distance from the edge of the cell to the two nearest base stations. Hence, the interference from farther base stations is weaker than the interference from the two nearest base stations by at least a factor of 2^n , where n is the propagation loss exponent. For typical values of n (3.8 to 4.0), this term is at least 12 dB. Hence, the overall interference is dominated by the contribution of the two nearest base stations. We therefore only consider inter-cell interference from the two neighboring sectors, sector 1 in cell C' , and sector 2 in cell C'' . However, all our results can be easily generalized to the case of multiple interfering sectors.

The signal received at the terminal is:

$$\mathbf{R}_t = \mathbf{S}_t + \mathbf{I}_t + \mathbf{N}_t,$$

where \mathbf{N}_t is the zero mean Gaussian noise at the receiver, and \mathbf{S}_t is the desired signal. We also have

$$\mathbf{S}_t = \mathbf{G}_0 A \sum_{n=-\infty}^{\infty} y_n h(t - nT_c) \cos \omega_0 t \quad (1)$$

where $y_n \in \{+1, -1\}$ is the transmitted symbol sequence, \mathbf{G}_0 is the forward link channel gain from the base station of serving sector 0 to the terminal, A is the signal amplitude, and $h(t)$ is a pulse (chip) of width T_c . In (1), $f_0 = \omega_0/2\pi$ is the carrier frequency, and we assume that $f_0 \gg 1/T_c$. Let T be the duration of a time slot. Referring to Fig. 2, the components with a bar are the matched filter outputs of the corresponding input components with a hat. Our objective is to determine the variance of the inter-cell interference component, $\bar{\mathbf{I}}$, so as to evaluate the SINR at the receiver.

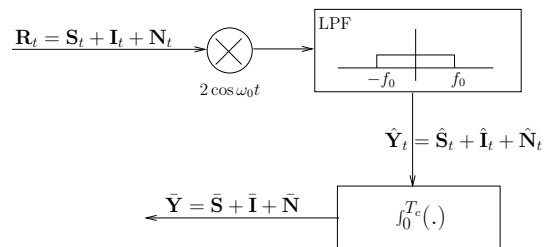


Fig. 2. Block diagram of a simple correlation receiver

We first consider inter-cell interference from a single interfering sector. Since the analysis dealing with the derivation of the variance of the inter-cell interference is technical in nature, we refer the reader to Appendix for the detailed derivation.

There, we show in (15) that the variance of the single inter-cell interference component is given by the following expression.

$$\sigma_I^2 = \frac{1}{3} \mathbf{G}_1^2 A^2 \rho_1 T_c^2, \quad (2)$$

where \mathbf{G}_1 is the channel gain from the base station of the interfering sector to the terminal and ρ_1 is the traffic load on the forward link of that sector. Or equivalently, ρ_1 is the probability that a time slot on the forward link of a sector is busy. Thus, the intensity of the forward link traffic in the neighboring sector has a role to play in determining the variance of the inter-cell interference. With multiple inter-cell interference components, we note that the data streams and the channel gains of different BSs are independent, and hence we can simply add the variance of each of the interference components. The variance due to noise, σ_N^2 , is simply $2N_0T_c$. The total variance of the output is

$$\sigma^2 = \frac{1}{3} A^2 T_c^2 (\mathbf{G}_1^2 \rho_1 + \mathbf{G}_2^2 \rho_2) + 2N_0 T_c, \quad (3)$$

where ρ_i is the forward link traffic load of the i th interfering sector. If we assume that the desired signal transmitted by the BS of sector 0 is $x(t) = Ah(t)$ (i.e., $y_0 = 1$ in (1)), then the mean of the output decision variable, m is:

$$\begin{aligned} m &= \int_0^{T_c} \mathbf{G}_0 Ah(t)h(t) dt \\ &= \mathbf{G}_0 AT_c \end{aligned}$$

Hence the SINR at the output of the filter is given by:

$$\text{SINR} = \frac{\mathbf{G}_0^2 A^2 T_c}{\frac{1}{3} A^2 T_c (\mathbf{G}_1^2 \rho_1 + \mathbf{G}_2^2 \rho_2) + 2N_0} \quad (4)$$

IV. NETWORK LOAD AND SINR

In the previous section we obtained an expression for the SINR at a terminal in presence of inter-cell interference from adjacent sectors. In the actual implementation of CDMA-HDR [13], the terminal measures the pilot signal transmitted periodically by the base station to determine the current SINR. This SINR value is then used to predict the supportable forward link data rate for that terminal for the next time slot. However, an important point to note in this scheme is that all the BSs are GPS-synchronized. Hence all the BSs transmit their pilot signal at the same time. Consequently, the SINR measured with respect to the pilot signal contains the worst case inter-cell interference, since the interfering signals are constantly ON during the measurement phase. Referring to (4), this amounts to measuring the SINR with $\rho_1 = \rho_2 = 1$.

To counter the over-estimation of interference (and also to counter fast fading), the CDMA-HDR system uses Hybrid-ARQ. In Hybrid-ARQ, packet lengths, and coding and modulation schemes are chosen intelligently to allow for early packet termination. Early packet termination refers to a successful reception of a packet before the nominal packet duration when the channel condition is good [10]. Hybrid-ARQ adjusts to network loading in the adjacent sectors, as well as to fast fading, and thereby results in a higher throughput in spite of initial conservative SINR estimates [13], [15]. However, we demonstrate that the gains of Hybrid-ARQ can

be improved substantially if it is provided with a more accurate initial estimate of the SINR. We propose an improved SINR estimation scheme that achieves this by taking into account the actual contribution of the inter-cell interference. We then discuss the benefits of the proposed scheme, and its impact on forward link scheduling and cell selection policy.

A. An improved scheme for SINR estimation

Referring to Fig. 1, consider a terminal located in sector 0, and assume that the terminal is being served by base station 0. Assume that in addition to BS 0, the terminal has BSs 1 and 2 are in its active set. The active set of a terminal is the set of BSs whose pilot signal can be correctly decoded by the terminal. The terminal receives inter-cell interference from sectors 1 and 2. Let α_i be the forward link SINR of sector i as measured by the terminal using the current scheme [13], [7] (i.e., by assuming 100% load in the rest of the sectors). Hence using (4),

$$\begin{bmatrix} \alpha_0 \\ \alpha_1 \\ \alpha_2 \end{bmatrix} = \begin{bmatrix} \frac{\mathbf{G}_0^2 A^2 T_c}{\frac{1}{3} A^2 T_c (\mathbf{G}_1^2 + \mathbf{G}_2^2) + 2N_0} \\ \frac{\mathbf{G}_1^2 A^2 T_c}{\frac{1}{3} A^2 T_c (\mathbf{G}_0^2 + \mathbf{G}_2^2) + 2N_0} \\ \frac{\mathbf{G}_2^2 A^2 T_c}{\frac{1}{3} A^2 T_c (\mathbf{G}_0^2 + \mathbf{G}_1^2) + 2N_0} \end{bmatrix} \quad (5)$$

In our proposed scheme, the terminal uses the above values of α_i that are known from pilot measurements. The above set of equations are then solved to obtain the channel gains \mathbf{G}_i as follows:

$$\begin{bmatrix} \mathbf{G}_0^2 \\ \mathbf{G}_1^2 \\ \mathbf{G}_2^2 \end{bmatrix} = \frac{2N_0}{A^2 T_c} \begin{bmatrix} 1 & -\frac{\alpha_0}{3} & -\frac{\alpha_0}{3} \\ -\frac{\alpha_1}{3} & 1 & -\frac{\alpha_1}{3} \\ -\frac{\alpha_2}{3} & -\frac{\alpha_2}{3} & 1 \end{bmatrix}^{-1} \begin{bmatrix} \alpha_0 \\ \alpha_1 \\ \alpha_2 \end{bmatrix} \quad (6)$$

Let the *actual* SINR at the terminal for the forward link of sector i be β_i . This SINR takes into account the traffic load in the interfering sectors. Using (4),

$$\begin{bmatrix} \beta_0 \\ \beta_1 \\ \beta_2 \end{bmatrix} = \begin{bmatrix} \frac{\mathbf{G}_0^2 A^2 T_c}{\frac{1}{3} A^2 T_c (\mathbf{G}_1^2 \rho_1 + \mathbf{G}_2^2 \rho_2) + 2N_0} \\ \frac{\mathbf{G}_1^2 A^2 T_c}{\frac{1}{3} A^2 T_c (\mathbf{G}_0^2 \rho_0 + \mathbf{G}_2^2 \rho_2) + 2N_0} \\ \frac{\mathbf{G}_2^2 A^2 T_c}{\frac{1}{3} A^2 T_c (\mathbf{G}_0^2 \rho_0 + \mathbf{G}_1^2 \rho_1) + 2N_0} \end{bmatrix} \quad (7)$$

Since \mathbf{G}_i are already known from (6), the actual SINR, β_i , for each of the sectors can be obtained by using the above expressions once ρ_i are known. Thus, we do not propose altering the current implementation of the pilot measurement procedure, and this makes our SINR estimation scheme easy to implement within the current framework.

However, we require that each base station keeps track of its forward link load ρ_i as follows. Since the derivation of (2) (see Appendix) only requires the probability that a time slot is busy, i.e., the value of ρ_1 , the load measurement scheme is very simple. Even with multi-slot packets, the load measurement scheme only needs to know whether a time slot was empty, or busy. A long term averaging exponential filter can then be used by each BS i to determine its average load as follows.

$$\hat{\rho}_i(n) = \alpha \cdot \mathbf{1}_{\{\text{time slot } n \text{ is busy.}\}} + (1 - \alpha) \cdot \hat{\rho}_i(n - 1) \quad (8)$$

In the above, $\mathbf{1}_{\{\cdot\}}$ is the indicator function, and $\alpha \in (0, 1)$ is chosen to match with the frequency of load updates. For

example, if we assume that the network load does not vary too much over an interval of 5 minutes, then the load is broadcast to the terminals once every 5 minutes ($1.8 \cdot 10^5$ time slots in CDMA-HDR), and the filtering parameter is tuned appropriately. Neighboring base stations periodically exchange the information about their current forward link load (over the high speed wired infrastructure) so that each base station knows the load in its neighboring interfering sectors. The base station periodically broadcasts this information to its users. If we assume that the traffic load over the forward link changes over the time scale of a few minutes, then the overheads of periodic load broadcasts are minimal. For bursty data applications, faster load updates can be used at the cost of increased control overheads. We understand that inaccuracy in load estimation can lead to over-estimation of SINR in the proposed scheme. However, this effect can be countered by making conservative load estimates. We believe that while this is an important issue, it is an implementation detail of the scheme, and hence not the focus of this paper.

Once the terminal has the information about the network loads in all the sectors that are in its active set, it can calculate the channel gains \mathbf{G}_i using (6), and the actual SINR values β_i using (7). It is easy to see that for low values of ρ_1 and ρ_2 , the actual contribution of inter-cell interference is much less, i.e., $\beta_0 > \alpha_0$. By using α_0 as the SINR estimate, the terminal reports a conservative data rate, and thereby gets lower throughput. Although Hybrid-ARQ can dynamically cope with SINR under-estimation, we argue that a more accurate initial estimate of SINR can only improve the user throughput. The extent of improvement will be illustrated through simulation results in Section V.

We label scheme A as the scheme that uses the worst case inter-cell interference estimate, i.e., the scheme that uses α_i as the SINR estimate, and also uses Hybrid-ARQ for early packet termination. This scheme is used in the current standards ([13], [7]). We label scheme B as the scheme that we propose above, i.e., the scheme that uses β_i as the SINR estimate, and also uses Hybrid-ARQ. In the next two sub-sections, we discuss the implications of using scheme B instead of scheme A on forward link scheduling and cell selection policy.

B. Inter-cell Interference and Scheduling

The fact that the terminals see a time-varying wireless channel over the forward link should be taken into account when scheduling data over the forward link. A class of scheduling policies called opportunistic scheduling policies ([13], [1], [5], [4]) have been proposed for maximizing the sector throughput by preferentially serving users with good channel condition. In all these works, as well as several other related works, no special consideration is given to the fact that the inter-cell interference has an important role to play in determining the SINR of a user. In the previous section, we saw that SINR estimation using scheme A has the disadvantage that it does not provide an accurate estimate of the inter-cell interference contribution in the SINR. Although this does not have an impact on the forward link opportunistic scheduling algorithm itself, it does have an impact on the

outcome of the scheduling decisions. This is because under scheme A, the users located near the cell boundary *report* a lower data rate than the actual supportable rate. Opportunistic scheduling algorithm usually favors users that *report* higher supportable rate. Thus, unless the scheduling discipline takes early termination due to Hybrid-ARQ into account, even the gains of Hybrid-ARQ could get affected by the scheduling policy. This is because opportunistic scheduling policies base their decisions on the reported inaccurate rate estimates. In section V, we present simulation results to illustrate that when opportunistic scheduling is used for serving users, scheme B provides better user throughput to the “poor” users than scheme A *without resulting in any degradation in the overall sector throughput*.

C. Inter-cell Interference and Cell Selection

When a user is about to hand over to a neighboring sector using cell-selection, it measures the SINR of all the BSs in its active set to determine the best serving sector. It is possible that due to geographical nearness, the pilot-aided SINR of the terminal for BS 0 is higher than that of BS 1, i.e., $\alpha_0 > \alpha_1$. However, the actual SINR of the terminal for BS 1 may be higher than that of BS 0, i.e., $\beta_1 > \beta_0$. Thus, the user will continue to stay in sector 0 instead of handing off to sector 1. We illustrate through simulation results that using α_i instead of β_i may result in sub-optimum cell selection, i.e., the resultant SINR of the terminal in the chosen cell may be lower when α_i are used as cell selection criterion instead of β_i .

V. SIMULATION RESULTS

A. Simulation setup

In this sub-section, we present an overview of the simulator (available for download [17]). A terminal receives forward link signals of two interfering sectors in its neighborhood. While it is easy to extend the simulation settings to account for more than two interfering sectors, we note that the signals of two neighboring sectors are substantially stronger than the interfering signal received from other distant sectors, and hence we simulate only two interfering sectors. Corresponding to each user, and each base station (serving base station as well as interfering base stations), a time-varying channel gain \mathbf{G}_i is generated in each time slot. The user SINR given by (4), is a function of \mathbf{G}_i , and \mathbf{G}_i^2 are random variables given by:

$$\mathbf{G}_i^2 = cd_i^{-n} \cdot 10^{\xi_i/10} \cdot \mathbf{W}_i^2 \quad (9)$$

In (9), the first term in the product is deterministic (for a fixed user location), and corresponds to path loss, while the second term is a random variable corresponding to log-normal shadowing loss. Here, ξ_i is a Gaussian random variable with mean 0, and variance σ_G . We use ITU path loss models for vehicular (120 kmph) and pedestrian (3 kmph) users [6]. Shadowing is correlated over each time slot depending on the speed of the user as per Gudmundson model [6]. Shadow correlation distance is the same for both vehicular and pedestrian models, and depends only on the environment (urban or suburban). Short term Rayleigh fading is accounted through \mathbf{W}_i , a Rayleigh distributed random variable. Time

Carrier frequency, f_0	2000 MHz
Log-normal Shadowing variance, σ_G	10 dB
Shadow correlation distance	20.0 m
Noise spectral density, N_0	-174 dBm/Hz
A, amplitude of transmit waveform (base station transmit power of 15W)	5.48
Chip duration, T_c (1.25 Mcps)	0.8 μ s
Radius of the sector, R	1 Km
R_0 for 90% cell coverage	$0.95R = 0.95$ Km
Miscellaneous gains: antenna gains, body loss, cable loss	15.2 dB
Building penetration loss, (only for pedestrian users)	12 dB
Pedestrian path loss in dB, $10 \log_{10}(cd^n)$ (f_0 in MHz, d in Km)	$30 \log_{10}(f_0) + 49 + 40 \log_{10}(d)$
Vehicular path loss in dB, $10 \log_{10}(cd^n)$ (f_0 in MHz, d in Km)	$21 \log_{10}(f_0) + 58.83 + 37.6 \log_{10}(d)$
Fraction of multi-path power captured by the receiver (vehicular user)	0.784

TABLE I
SIMULATION SETTINGS

correlation of Rayleigh fading is determined by the speed of the terminal, and is simulated by using the Filtered Gaussian Noise technique from [11]. Simulation parameters are listed in Table I, and have been taken from [6], [13]. Each simulation is run for 20,000 time slots, and 600 independent simulations are run to gather user throughputs within 90% confidence interval.

We select user locations so that the terminal is equidistant from the two interfering base stations. For measuring distances relative to the size of the cell, user locations are selected to be multiples of R_0 , where R_0 corresponds to 90% cell coverage radius, i.e., the area of a sector of radius R_0 is 90% of the area of a sector of radius R . It is easy to show that $R_0 = 0.95R$. In our case, the cell radius R is 1 Km, and hence R_0 equals 0.95 Km.

Table II shows the SINR to data rate mapping for a maximum packet error rate of 1% (taken from [10], [13]). If the average SINR over the duration of the packet transmission is lower than the required threshold, then the packet is assumed to be lost as in [2]. Each type of packet corresponds to a different coding/modulation scheme, and is transmitted over a certain nominal number of time slots (1, 2, 4, 8, 16). In a real system [13], multi-slot packet interleaving at the physical layer is used for better time diversity, wherein a multi-slot packet is transmitted over inter-spaced slots instead of consecutive slots. We simulate this multi-slot interleaving of packets in our simulator. A real system also uses Hybrid-ARQ for early termination of packets if the channel is better than predicted. We implement Hybrid-ARQ functionality in our simulator. As in [10], we assume that a packet of nominal length of N slots terminates in m slots ($N > m$), if the average SINR during the first m slots of that packet transmission is greater than the threshold SINR required for early termination within m slots for that packet type. The required SINR values for early termination for different packet types are taken from Table 4 in [10].

At each terminal, we also simulate the SINR prediction

scheme as used in the CDMA-HDR system [12]. In this scheme, the terminal has an averaging filter bank for each packet type. The filter bank uses the SINR measurements from the past to predict the future SINR for each packet type. For a vehicular user, the prediction method essentially uses long term averaging of the past SINR samples over the duration of the packet length. For pedestrian users, the filter bank computes a zero mean short term average of the SINR that is added to the above long term average. This short term average tracks the current channel condition. The pedestrian channel changes a relatively slowly as compared to the vehicular channel, and hence in addition to the long term average, short term averaging is also used. In our simulator, we implement the above SINR prediction scheme. See [12] for the implementation details of this channel prediction scheme. In a real CDMA-HDR network, in addition to the above SINR prediction algorithm, there is a control loop that adjusts the predicted SINR values based on measured packet error rate. If the measured packet error rate is high, then the terminal makes its subsequent SINR predictions more conservative. However, we do not implement this strategy in our simulator, since there are several parameters involved in fine tuning of such a dynamic control loop. However, we fine tune the parameters of the basic SINR estimation scheme in [12] for getting acceptable packet error rates. We also simulate the proportional fair scheduling algorithm from [13] when there are multiple users in the system.

B. Simulation results

In all our simulations, although the time variations of the user channel as a function of user speed have been simulated (time-varying shadowing and fading), we assume that *the user does not change its location during the course of the simulation*. In other words, the path loss component of the channel gain remains unchanged during the course of the simulation. This is because the objective of our study is to demonstrate that the users located near the boundary of the cell benefit from our proposed scheme. Such an approach is often used by the network designers to study how throughput degrades as a function of the distance of the user from the serving base station. This is unlike the simulation results presented in [13], where the user location actually changes during the course of the simulation. In all the simulations, we assume for simplicity that the network loads in both the interfering sectors are the same, i.e., $\rho_1 = \rho_2 = \rho$, and we vary ρ to study the throughput gains of scheme B over scheme A for different network loads in the interfering sectors. In the simulations, the loading ρ is modeled as an ON/OFF transmission in every time slot, and the ON event is determined by sampling a uniformly distributed random variable. In the simulations, we also assume that the events of receiving interference over successive slots are independent. However our scheme can easily take into account time correlated interference process by estimating ρ_i using (8).

1) *Single user throughput*: For these simulations, we assume that there is a single user in the system (multiple user scenario is presented later), and the base station has infinite

Data rate (kb/s)	38.4	76.8	153.6	307.2	614.4	921.6	1228.8	1843.2	2457.6
SINR (dB)	-11.5	-9.2	-6.5	-3.5	-0.5	2.2	3.9	8.0	10.3

TABLE II

SINR TO DATA RATE MAPPING FOR 1% PACKET ERROR RATE.

number of data packets to be sent over the forward link to this user. We simulate the single user case to compare the user throughput for schemes A and B for both pedestrian as well as vehicular models. In Fig. 3, we plot the throughput when the interfering sectors are fully loaded, i.e., $\rho_1 = \rho_2 = 1.0$. We refer to this case as the base case, since we expect that neither Hybrid-ARQ, nor the knowledge of interfering network load, can result in any throughput improvements by countering inter-cell interference. We note from Fig. 3 that near the cell boundary, the vehicular throughput degrades more rapidly than the pedestrian throughput. This is because inter-cell interference is more serious in vehicular model due to a lower path loss exponent.

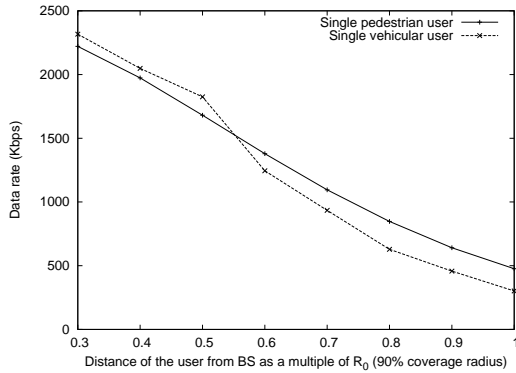


Fig. 3. Data rate with a single user in the system and with fully loaded interfering sectors, i.e., $\rho_1 = \rho_2 = \rho = 1.0$ (base case).

We first study the pedestrian model. In Fig. 4(a), we plot the percentage throughput improvement of scheme A over the base case of Fig. 3. The gain in throughput over the base case is up to about 12%, and is due to Hybrid-ARQ adjusting to inter-cell interference. In Fig. 4(b), we plot the percentage throughput improvement when scheme B is used for SINR estimation. This gain, which is up to about 50%, is due to Hybrid-ARQ, as well as due to a more accurate initial estimation of SINR. We can clearly see that although Hybrid-ARQ results in throughput improvement, the gains are substantially higher when scheme B is used along with Hybrid-ARQ. This is because the proposed scheme provides Hybrid-ARQ a more accurate initial estimate (as a function of the interfering network load) around which to perform subsequent fine tuning of the data rate. Due to space constraints, we do not present results on packet error rates. However, the packet error rates were below 1% for both the schemes for these settings (except near the edge of the cell, where the error rates were slightly higher, but still below 2%).

In Fig. 5, we plot the percentage throughput improvement of schemes A and B over the base case for vehicular model. It is well-known that vehicular users are more interference dominated than noise dominated [13]. As a result, better

estimation of inter-cell interference benefits vehicular users more than pedestrian users. Comparing Fig. 4(a) and Fig. 5(a), we note that the gains due to Hybrid-ARQ with scheme A are higher for vehicular model than pedestrian model. We note that in Fig. 5(a), Hybrid-ARQ allows scheme A to achieve a data rate that is up to 40% higher than the base case. These results agree with the results obtained in [15], [13], where the authors show that Hybrid-ARQ results in throughput improvements in presence of inter-cell interference. We also note from Fig. 5(b), that when scheme B is used along with Hybrid-ARQ up to 100% throughput improvement is obtained over the base case. With both the schemes, for almost all the settings the packet error rates were under 1%, and never above 2%. We do not present the results on packet error rates due to space constraints. Thus the proposed scheme enhances the functioning of Hybrid-ARQ by providing more accurate initial SINR estimates. Finally, we plot the percentage improvement of scheme B over scheme A in Fig. 6(a) and Fig. 6(b). We note that the proposed scheme substantially outperforms the currently implemented scheme, and the gains are especially higher in the case of vehicular users, and users near the cell boundary. For example, at a distance of $0.8R_0 = 760\text{m}$, and with an interfering network load of 0.5, the proposed scheme results in 35% improvement in the throughput of a vehicular user, and 15% improvement in the throughput of a pedestrian user.

2) *Multiple users with opportunistic scheduling:* In this subsection we present simulation results when three users are served over the forward link. The users are located at distances $0.4R_0$, $0.7R_0$ and $1.0R_0$ from the serving base station. We simulate the proportional fairness scheduling discipline from [13]. We run two sets of simulations. In the first set, all the three users have pedestrian channel model, while in the second set, all the users have vehicular channel model.

In Fig. 7, we plot the throughput received by each user as a function of the interfering network load under schemes A and B for pedestrian model. We note that as the interfering network load decreases, both the schemes result in higher throughput for users 2 and 3. With scheme A, even the throughput of user 1 increases with decreasing network load. However, with scheme B, the throughput of user 1 decreases marginally with decreasing network load. We observe this behavior because both the schemes are designed to improve the throughput of a user when the inter-cell interference is lower. However this benefit is especially more pronounced for users located near the cell boundary (users 2 and 3). Note that the SINR estimation scheme and Hybrid-ARQ interact with the opportunistic scheduling discipline in a non-trivial way. In presence of opportunistic scheduling discipline, scheme B benefits users 2 and 3 while penalizing user 1 marginally. However note from Fig. 9(a) that scheme B always results in

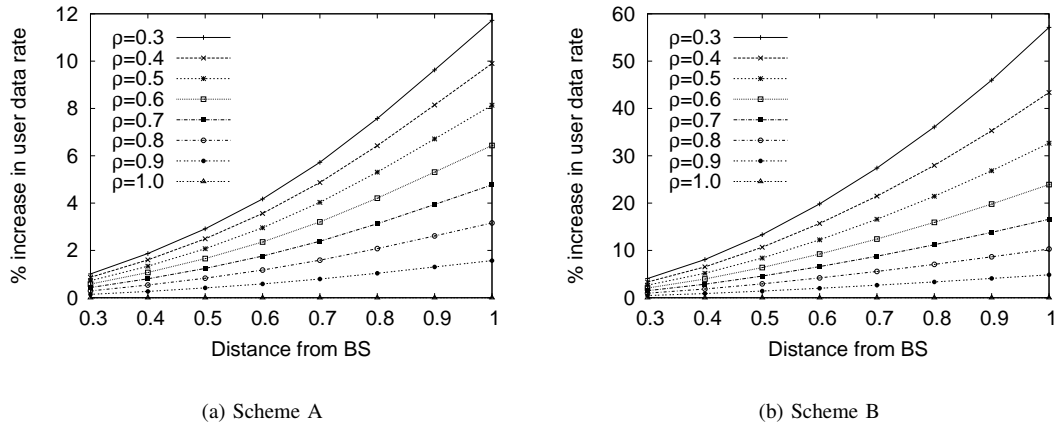


Fig. 4. Gain in throughput of a single pedestrian user as compared to base case (throughput for pedestrian model in Fig. 3).

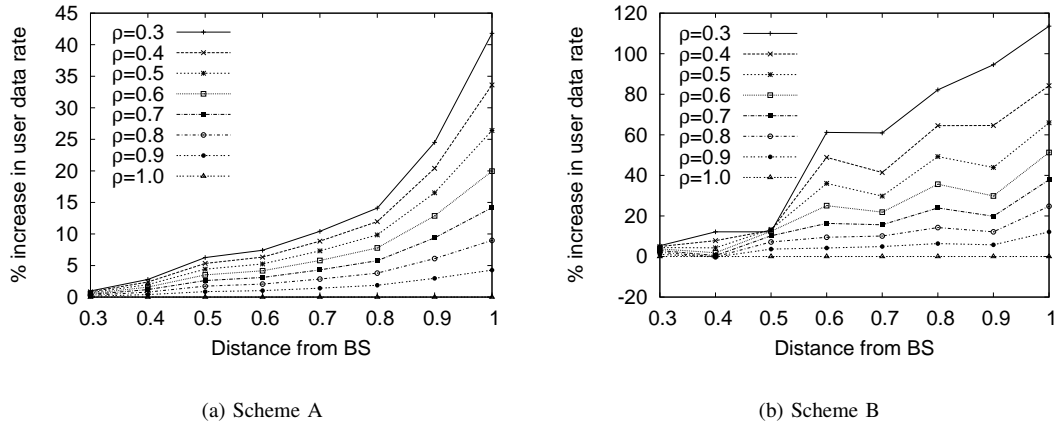


Fig. 5. Gain in throughput of a single vehicular user as compared to base case (throughput for pedestrian model in Fig. 3).

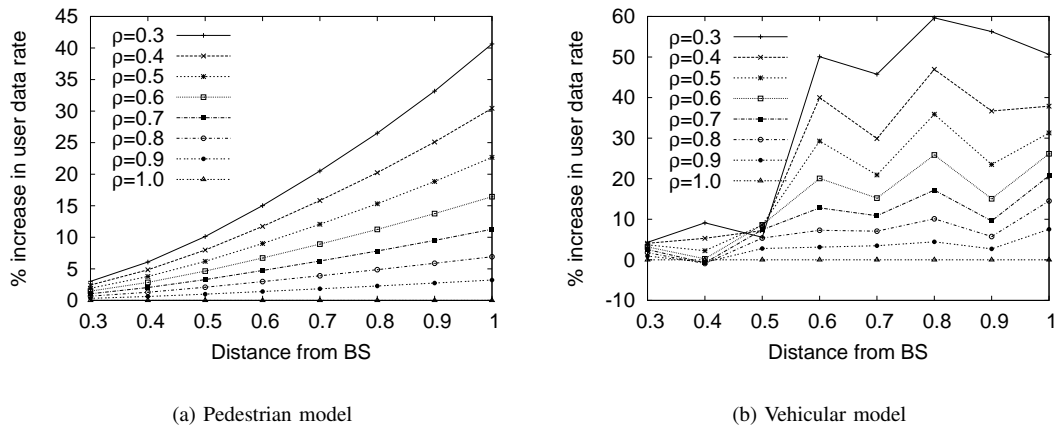


Fig. 6. Percentage improvement of scheme B over scheme A.

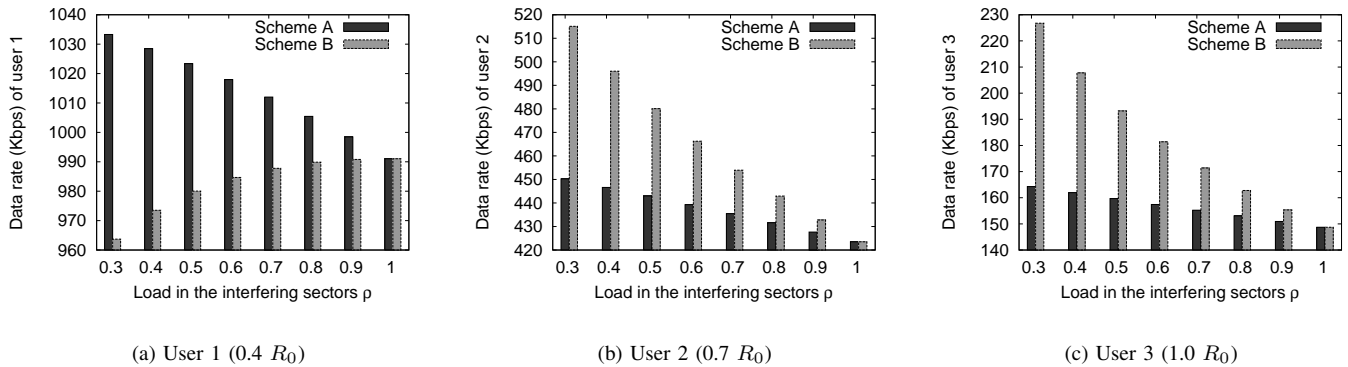


Fig. 7. Throughputs of all the users with pedestrian channel model.

a higher overall sector throughput than scheme A. We observe similar results for the vehicular model in Fig. 8 and Fig. 9(b), but the throughput improvement of users 2 and 3 is even higher in the vehicular case than the pedestrian case. Thus, the proposed scheme benefits the “poor” users, i.e., users located far from the serving base station (users 2 and 3), without degrading the overall sector throughput.

3) *Proposed scheme and cell selection policy*: In these set of simulations we illustrate that using scheme A for SINR estimation (i.e., using α_i as SINR estimates) instead of scheme B (i.e., using β_i as SINR estimates) may result in sub-optimum cell selection. We simulate a scenario in which a vehicular user is located at a distance of $1.0R_0$ from BS 0, and is equidistant from BS 1 and BS 2. The network loads in the three sectors are $\rho_0 = 0.3$, $\rho_1 = 1.0$, $\rho_2 = 0.3$. These load values have been specifically chosen to illustrate that although the terminal is geographically closest to BS 0 (and hence $\alpha_0 > \alpha_1, \alpha_2$), the effect of network loading results in actual SINRs β_i such that $\beta_1 > \beta_0, \beta_2$. This can be seen from Fig. 10 where we plot α_0 , α_1 , β_0 and β_1 after time averaging them over over the past 0.5 seconds. Typically, instantaneous SINR estimates are time averaged over a few seconds in handoff policies (see [14]). If β_i is used for making cell selection decisions, then the terminal would handoff to sector 1 instead of staying in sector 0, and would thereby have a higher SINR (β_1). Thus the proposed scheme can prove beneficial to users during cell selection.

VI. CONCLUSIONS

We study the problem of characterizing inter-cell interference in cellular data networks. We note that the inter-cell interference experienced by a terminal in a given sector is a function of the network load on the forward link of the neighboring sectors. We propose an improved scheme to estimate the SINR at a terminal, so that the measurements take into account the actual (and not the worst case) inter-cell interference. Our proposed scheme requires the base stations to use traffic measurement (forward link network load), and send this information to the terminals. The terminals then use this information along with an improved SINR estimation scheme, to obtain an accurate estimate of their current channel state. Through simulations, we show that the proposed scheme outperforms the current SINR estimation scheme by providing

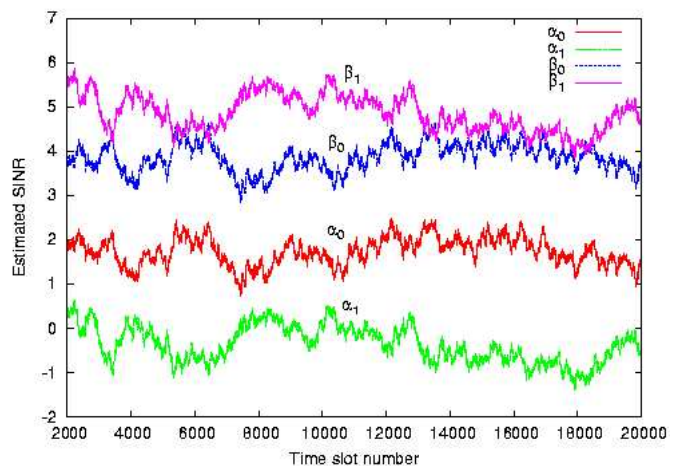


Fig. 10. Predicted SINR for cells 0 and 1 under schemes A and B.

higher throughput to users, especially the users located farther from the serving base station. We also observe that the gains of the proposed scheme are more pronounced for vehicular users than pedestrian users. The proposed scheme also benefits users in making cell selection choices during handoffs.

APPENDIX I PROOFS OF MISCELLANEOUS RESULTS

In this Appendix, we determine the variance of the inter-cell interference component, $\bar{\mathbf{I}}$ in Fig. 2. Consider a single inter-cell interference component, i.e., $\mathbf{I}_t = \mathbf{I}_t^1$. Note that \mathbf{I}_t^1 is the stochastic process corresponding to the forward link signal in the interfering sector *as seen by a terminal* in the given sector. However, we know that the terminal synchronizes itself with its serving base station, and hence there is a location dependent random time and the phase delay between the received signals of the serving BS and the interfering BS. Let θ be this random time delay, and let ϕ be the random phase delay. We also know that all the BSs are GPS synchronized, and hence the time and phase delays observed by the terminal between the received signals from two BSs are entirely due to the different propagation path lengths from different BSs. Let \mathbf{Z}_t be the baseband portion of the *actual* signal transmitted

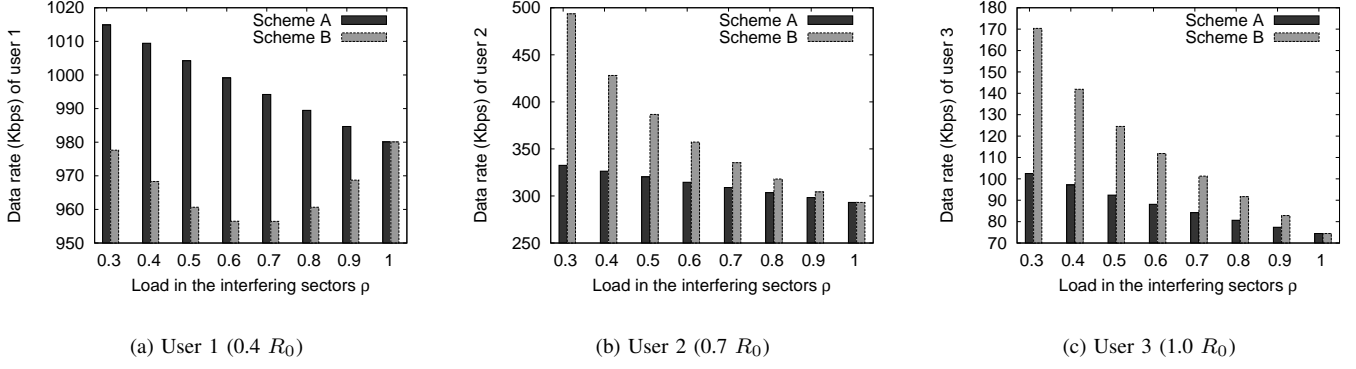
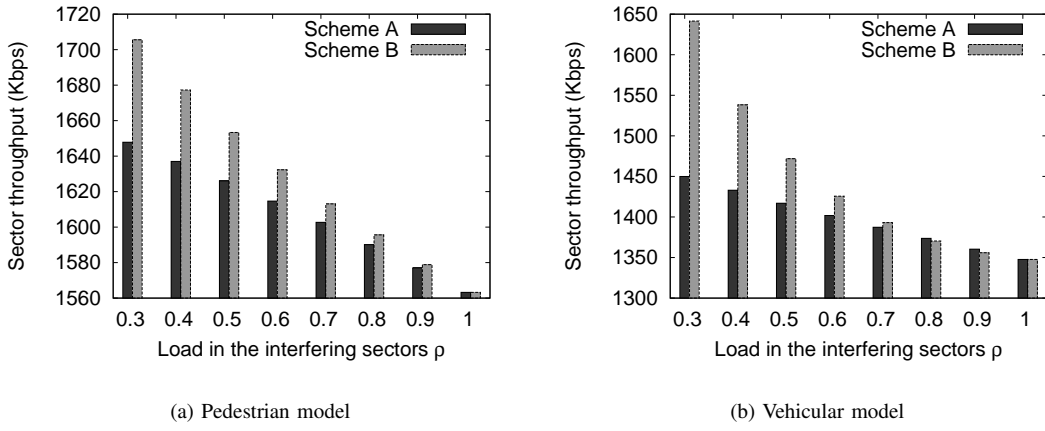


Fig. 8. Throughputs of all the users with vehicular channel model.

Fig. 9. Sector throughput with user 1 located at $0.4R_0$, user 2 at $0.7R_0$, user 3 at $1.0R_0$.

by the interfering BS. The signal \mathbf{I}_t^1 received by the terminal is $\mathbf{I}_t^1 = \mathbf{G}_1 \mathbf{Z}_{t-\theta} \cos(\omega_0 t + \phi)$, where \mathbf{G}_1 is the channel gain from BS 1 to the terminal. After frequency down-conversion, and low pass filtering, the resultant signal $\hat{\mathbf{I}}_t$ is:

$$\hat{\mathbf{I}}_t = \mathbf{G}_1 \mathbf{Z}_{t-\theta} \cos \phi \quad (10)$$

Note that θ and ϕ are random variables independent of each other as well as \mathbf{Z}_t . We also assume that ϕ is uniformly distributed over $(0, 2\pi]$, and $(\theta \bmod T_c)$ is uniformly distributed over the chip interval $(0, T_c]$.

The latter assumption is justified because typical CDMA settings [13] have a sector radius of the order of 1 Km. As a result, path difference is of the order of few hundred meters, and so the random delay θ is of the order of a few μs , while T_c is $0.8 \mu s$. Note that we are only concerned with $(\theta \bmod T_c)$, since the stream of symbols transmitted by the interfering BS appears like a random sequence of symbols to the terminal, and hence only delay modulo T_c matters. Henceforth we drop ‘mod T_c ’.

We now prove that \mathbf{Z}_t is a wide sense cyclostationary stochastic process (WSCS), and $\hat{\mathbf{I}}_t$ is a wide sense stationary process. Since \mathbf{Z}_t is the actual forward link traffic of the interfering sector (synchronized to the system GPS clock), we

have

$$\mathbf{Z}_t = \sum_{n=-\infty}^{\infty} z_n A h(t - nT_c), \quad (11)$$

where $h(\cdot)$ is the symbol waveform (a pulse of width T_c), and z_n are random variables taking values in the set $\{1, -1, 0\}$. The case of $z_n = 0$ corresponds to the chip of an idle time slot of the forward link during which no data is sent, while $z_n = \{1, -1\}$ corresponds to the chip of a busy time slot of the forward link of the interfering sector. Let ρ_1 be the network load on the forward link of the interfering sector, i.e., ρ_1 is the probability that a time slot on the forward link of the interfering sector is busy.

Proposition 1: For the sequence z_n in (11),

$$\mathbf{E}[z_n z_m] = \rho_1 \cdot \delta_{m,n},$$

where $\delta_{m,n}$ is 1 if $m = n$, and 0 otherwise.

Proof: It is possible to think of \mathbf{Z}_t as a product of two independent stochastic processes: Process \mathbf{U}_t which corresponds to the actual traffic in each time slot, and \mathbf{V}_t which corresponds to an i.i.d. random bit sequence taking

values $\{1, -1\}$. We can write:

$$\mathbf{Z}_t = A\mathbf{U}_t\mathbf{V}_t,$$

$$\mathbf{U}_t = \sum_{k=-\infty}^{\infty} u_k g(t - kT), \quad \mathbf{V}_t = \sum_{n=-\infty}^{\infty} v_n h(t - nT_c)$$

In the above equations, \mathbf{U}_t is a stochastic process that is either 0 or 1 in each time slot (of length T) depending on whether a packet is transmitted over the forward link, i.e., u_k are random variables (not necessarily i.i.d.) taking values in $\{0, 1\}$. Each time slot represented by $g(t)$, is a pulse of width T . The actual bit-stream of the packet which corresponds to the chip sequence within a busy time slot is represented by \mathbf{V}_t . Each chip represented by $h(t)$, is a pulse of width T_c . Also note that v_n are i.i.d. random variables taking values in $\{1, -1\}$. Let $T/T_c = M$ be the number of chips per time slot. When the time slot is idle, $\mathbf{Z}_t = 0$ thanks to $\mathbf{U}_t = 0$, and hence \mathbf{V}_t does not matter. Also note that $z_n = u_{k_n}v_n$, and $k_n = \lfloor \frac{n}{M} \rfloor$, where $\lfloor \cdot \rfloor$ is the floor function. Since the actual busy period of the forward link is independent of the value of the chip sequence, we can safely assume that \mathbf{U}_t and \mathbf{V}_t are independent. Since $z_n = u_{k_n}v_n$, we can write

$$\begin{aligned} \mathbf{E}[z_n z_m] &= \mathbf{E}[(u_{k_n}v_n)(u_{k_m}v_m)] \\ &= \mathbf{E}[u_{k_n}^2] \cdot \delta_{m,n}, \end{aligned}$$

since u_i and v_j are independent, and v_j are i.i.d. on $\{-1, 1\}$. Thus,

$$\mathbf{E}[z_n z_m] = \rho_1 \cdot \delta_{m,n},$$

since $\mathbf{E}[u_{k_n}^2] = P\{u_{k_n} = 1\} = \rho_1$. We have used the fact that $P\{u_k = 1\}$ is the probability that the time slot is busy, which is equal to ρ_1 , the network load on the forward link. ■

Proposition 2: The stochastic process \mathbf{Z}_t in (11) is wide sense cyclostationary (WSCS), and

$$R_{ZZ}(t + \tau, t) = A^2 \rho_1 \sum_{n=-\infty}^{\infty} h(t + \tau - nT_c)h(t - nT_c). \quad (12)$$

Proof: Using the approach of Proposition 1, it is easy to see that $\mathbf{E}[z_n] = 0$, and hence $\mathbf{E}[\mathbf{Z}_t] = 0$. The autocorrelation function of \mathbf{Z}_t is given by:

$$\begin{aligned} R_{ZZ}(t + \tau, t) &= \mathbf{E}[\mathbf{Z}_{t+\tau}\mathbf{Z}_t] \\ &= A^2 \sum_{n=-\infty}^{\infty} \sum_{m=-\infty}^{\infty} \mathbf{E}[z_n z_m] h(t + \tau - nT_c) \times \\ &\quad h(t - mT_c) \\ &= A^2 \rho_1 \sum_{n=-\infty}^{\infty} h(t + \tau - nT_c)h(t - nT_c), \end{aligned} \quad (13)$$

where ρ_1 is the traffic intensity in the interfering sector, and we used Proposition 1 in the last step.

From (13), we note that $R_{ZZ}(t + \tau, t)$ is periodic with a period T_c . We also have $\mathbf{E}[\mathbf{Z}_t] = 0$. Thus \mathbf{Z}_t is a wide sense cyclostationary process since its mean and autocorrelation are periodic with period T_c (see [8], pp. 373). ■

Proposition 3: The stochastic process $\hat{\mathbf{I}}_t$ in (10), i.e., $\hat{\mathbf{I}}_t = \mathbf{G}_1 \mathbf{Z}_{t-\theta} \cos \phi$, is wide sense stationary with mean zero and auto-correlation function given by:

$$R_{\hat{I}\hat{I}}(\tau) = \frac{\mathbf{G}_1^2 A^2 \rho_1}{2} \left(1 - \frac{|\tau|}{T_c}\right) \mathbf{1}_{\{|\tau| \leq T_c\}} \quad (14)$$

where $\mathbf{1}_{\{\cdot\}}$ is the indicator function.

Proof: We know that $\hat{\mathbf{I}}_t$ is a delayed version of \mathbf{Z}_t , and the delay is randomly and uniformly distributed over $(0, T_c]$. Note that multiplication by an independent random variable $\cos \phi$ which is not time-varying, does not impact the wide sense stationary nature of $\hat{\mathbf{I}}_t$. Hence using Theorem 2 in [8], pp. 374, we conclude that $\hat{\mathbf{I}}_t$ is a wide sense stationary process, and the mean and the autocorrelation function of $\hat{\mathbf{I}}_t$ are given by:

$$\begin{aligned} \mathbf{E}[\hat{\mathbf{I}}_t] &= \mathbf{G}_1 \left\{ \frac{1}{T_c} \int_0^{T_c} \mathbf{E}[\mathbf{Z}_t] dt \right\} \mathbf{E}[\cos \phi], \\ R_{\hat{I}\hat{I}}(\tau) &= \mathbf{G}_1^2 \left\{ \frac{1}{T_c} \int_0^{T_c} R_{ZZ}(t + \tau, t) dt \right\} \mathbf{E}[\cos^2 \phi] \end{aligned}$$

Since ϕ is uniform over $(0, 2\pi]$, $\hat{\mathbf{I}}_t$ is zero mean. Substituting $R_{ZZ}(t + \tau, t)$ from (12) and integrating,

$$R_{\hat{I}\hat{I}}(\tau) = \frac{\mathbf{G}_1^2 A^2 \rho_1}{2} \left(1 - \frac{|\tau|}{T_c}\right) \mathbf{1}_{\{|\tau| \leq T_c\}}$$

where $\mathbf{1}_{\{\cdot\}}$ is the indicator function. ■

Having obtained $R_{\hat{I}\hat{I}}(\tau)$, we can now determine the variance of the inter-cell interference component, $\bar{\mathbf{I}}$, at the output of the filter. From Proposition 3 we know that $\hat{\mathbf{I}}_t$ is zero mean. Hence the corresponding matched filter output $\bar{\mathbf{I}}$ is also zero mean. Since the impulse response of the matched filter is $h(t)$, using (14) we obtain the variance of $\bar{\mathbf{I}}$ as follows:

$$\begin{aligned} \sigma_{\bar{\mathbf{I}}}^2 &= \int_{-\infty}^{\infty} \int_{-\infty}^{\infty} h(\tau_1)h(\tau_2)R_{\hat{I}\hat{I}}(\tau_1 - \tau_2) d\tau_1 d\tau_2 \\ &= \int_0^{T_c} \int_0^{T_c} R_{\hat{I}\hat{I}}(\tau_1 - \tau_2) d\tau_1 d\tau_2 \\ &= \frac{1}{3} \mathbf{G}_1^2 A^2 \rho_1 T_c^2 \end{aligned} \quad (15)$$

ACKNOWLEDGMENTS

This work was supported in part by the Indiana Twenty First Century Fund through the Indiana Center for Wireless Communication and Networking, and by the National Science Foundation Grant No. 0087266. We would also like to thank the anonymous reviewers for their insightful comments and suggestions that enabled us to substantially improve the quality of this manuscript.

REFERENCES

- [1] P. Bender, P. Black, M. Grob, R. Padovani, N. Sindhushyana, and A. Viterbi. CDMA/HDR: A bandwidth-efficient high-speed wireless data service for nomadic users. *IEEE Communications Magazine*, 38(7):70–77, 2000.
- [2] S. Chakravarty, R. Pankaj, and E. Esteves. An algorithm for reverse traffic channel rate control for CDMA2000 high rate packet data systems. In *Proceedings of IEEE Globecom*, 2001.

- [3] H. Haas and S. McLaughlin. A derivation of the pdf of adjacent channel interference in a cellular system. *IEEE Communications Letters*, 8(2):102–104, February 2004.
- [4] S. S. Kulkarni and C. P. Rosenberg. Opportunistic scheduling generalizations to include multiple constraints, multiple interfaces, and short term fairness. To appear in *Special issue of ACM/Kluwer Wireless Network Journal (WINET)*.
- [5] X. Liu, E. K. P. Chong, and N. B. Shroff. Transmission scheduling for efficient wireless utilization. In *Proceedings of IEEE INFOCOM*, 2000.
- [6] ITU-MTR M.1225. *Guidelines for evaluation of radio transmission technologies for IMT-2000*, 2000.
- [7] 3GPP2 Document no. C.S0002-D v1.0. *Physical Layer Standard for cdma2000 Spread Spectrum Systems - Revision D*, Feb 2004. Located at http://www.3gpp2.org/Public_html/specs/C.S0002-D_v1.0_021704.pdf.
- [8] A. Papoulis. *Probability, Random Variables and Stochastic Processes*. McGraw-Hill, 1991.
- [9] J. M. Romero-Jerez, M. Ruiz-Garcia, and A. Diaz-Estrella. Interference statistics of cellular DS/CDMA systems with base station diversity under multipath fading. *IEEE Transactions on Wireless Communications*, 2(6):1109–1113, November 2003.
- [10] N. T. Sindhushayana and P. J. Black. Forward link coding and modulation for CDMA2000 1xEVDO (is-856). In *Proceedings of The 13th IEEE International Symposium on Personal, Indoor and Mobile Radio Communications*, 2002.
- [11] G. L. Stuber. *Principles of Mobile Communication*. Kluwer Academic Publishers, 2001.
- [12] Q. Wu, P. J. Black, and N. T. Sindhushayana. System and method for accurately predicting signal to interference and noise ratio to improve communications system performance. *United States Patent: 6426971*, July 2002. Available at United States Patent and Trademark Office <http://www.uspto.gov>.
- [13] Q. Wu and E. Esteves. The cdma2000 high rate packet data system. *Chapter 4 of Advances in 3G Enhanced Technologies for Wireless Communications*, March 2002. Editors: Jiangzhou Wang and Tung-Sang Ng.
- [14] M. Chopra, K. Rohani and J. Reed. Analysis of CDMA range extension due to soft handoff. *Proc. IEEE VTC*, Chicago, IL, July 1995, pp. 917–921.
- [15] Q. Bi. A Forward Link Performance Study of the 1xEV-DO Rev. 0 System Using Field Measurements and Simulations. Lucent Technologies, March 2004. White paper available at http://www.cdg.org/resources/white_papers.asp.
- [16] Y. C. Yoon. An improved Gaussian approximation for probability of bit-error analysis of asynchronous bandlimited DS-CDMA systems with BPSK spreading. *IEEE Transactions on Wireless Communications*, 1(3):373–382, July 2002.
- [17] V. Mhatre and C. Rosenberg. “A simulator for CDMA-HDR data networks with Hybrid-ARQ and opportunistic scheduling functionality,” available at http://min.ecn.purdue.edu/~mhatre/cdmahdr_sim.tar.gz.



Vivek P. Mhatre Vivek P. Mhatre received a PhD in Electrical Engineering from Purdue University, West Lafayette, IN, USA in May 2005. Since then, Vivek has been working as a Postdoctoral Fellow at Intel Research Labs, Cambridge, UK. He was a visiting researcher at the University of Waterloo, Canada from September 2004 to November 2004. He received his Bachelors degree (B.Tech) in Electrical Engineering from Indian Institute of Technology, Bombay, India, in August 2000.

Vivek’s interests lie broadly in the area of wireless communications. He is interested in problems of interference modeling and QoS in cellular networks, Roaming, MAC tuning and network design of 802.11 wireless networks, as well as design and dimensioning of wireless sensor networks. He has worked on both, analytical modeling, as well as system building aspects of wireless networks.



Catherine P. Rosenberg Professor Rosenberg received the Diplome d’Ingenieur degree from Ecole Nationale Supérieure des Telecommunications de Bretagne, Brest, France, in 1983. She received her M.S. (Comp. Sci.), from University of California at Los Angeles in 1984, and the Doctorat en Sciences degree from , Université de Paris XI, Orsay, France.

From 1984–86 Professor Rosenberg was an engineer with ALCATEL, Lannion, France. From 1987–1988 she was a Member of Technical Staff at AT&T Bell Labs., Holmdel, N.J. From 1988–1996, she was

Associate Professor at the Department of Electrical and Computer Engineering, Ecole Polytechnique, Montreal, Canada. She was with Nortel Networks Harlow, UK from September 1996 to July 1999. She created and headed the R&D Department in Broadband Satellite Networking. She was also a Visiting Professor in the Department of Electrical and Electronics Engineering at Imperial College, London till January 2000. Catherine Rosenberg joined the faculty of the School of Electrical and Computer Engineering at Purdue University in August 1999 as Associate Professor with tenure. She was promoted to Full Professor in Summer 2002. From May 2002 to August 2004, she was the Director of the Center for Wireless Systems and Applications (CWSA) at Purdue University. She joined University of Waterloo on Sept 1st, 2004 as the Chair of the Department of Electrical and Computer Engineering. She also holds a University Research Chair.

Catherine Rosenberg has been a consultant (“expert scientifique”) to CNET (France -Telecom) from January 1994 to September 1996 and acts as an expert/consultant for different companies and institutions. She was an Associate Editor for IEEE Communications Magazine and Telecommunications Systems, and is now an Associate Editor for IEEE Transactions on Mobile Computing, IEEE Communications Surveys and Series co-Editor for the Series on Adhoc and Sensor Networks for IEEE Communications Magazine. She has been and is involved in many conferences including IEEE Infocom, IEEE Globecom, International Teletraffic Congress (ITC) and IFIP Broadband Communication. She has authored over 70 papers on broadband and wireless networking and traffic engineering and has filed several patents.

Professor Rosenberg’s research interests span wireless networks, broadband multimedia networks (IP, ATM, etc.), resource management, network optimization (design and routing), QoS and multicast, traffic engineering, pricing.